

1 **IL-10 and ICOS differentially regulate T cell responses in the brain during chronic**  
2 ***Toxoplasma gondii* infection**

3

4 Carleigh A. O'Brien\*, Samantha J. Batista\*, Katherine M. Still\*, and Tajie H. Harris\*

5

6 Affiliations: \*Center for Brain Immunology and Glia, Department of Neuroscience, University of  
7 Virginia, Charlottesville, VA 22908

8

9 Corresponding Author:

10 Tajie H. Harris, MR-4 Room 6148, 409 Lane Road, Charlottesville, VA 22908

11 Phone: 434-982-6916

12 Fax: 434-9824380

13 Email: [tajieharris@virginia.edu](mailto:tajieharris@virginia.edu)

14

15 This work was funded by the National Institutes of Health grants R01NS091067 to T.H.H.,  
16 T32AI007496 to C.A.O, T32AI007046 to S.J.B., and T32GM008328 to K.M.S., as well as the  
17 University of Virginia Robert R. Wagner Fellowship to C.A.O.

18

19

20

21

22

23

24

25 **Abstract**

26 Control of chronic CNS infection with the parasite *Toxoplasma gondii* requires an ongoing T cell  
27 response in the brain. Immunosuppressive cytokines are also important for preventing lethal  
28 immunopathology during chronic infection. To explore the loss of suppressive cytokine exclusively  
29 during the chronic phase of infection we blocked IL-10 receptor (IL-10R). Blockade was associated with  
30 widespread changes in the inflammatory response, including increased antigen presenting cell (APC)  
31 activation, expansion of CD4<sup>+</sup> T cells, and increased neutrophil recruitment to the brain, consistent with  
32 previous reports. We then sought to identify regulatory mechanisms contributing to IL-10 production,  
33 focusing on ICOS (inducible T cell costimulator), a molecule that promotes IL-10 production in many  
34 systems. Unexpectedly, ICOS-ligand (ICOSL) blockade led to a local expansion of effector T cells in the  
35 inflamed brain without affecting IL-10 production or APC activation. Instead, we found that ICOSL  
36 blockade led to changes in T cells associated with their proliferation and survival. Specifically, we  
37 observed increased expression of IL-2 associated signaling molecules, including CD25, STAT5  
38 phosphorylation, Ki67, and Bcl-2 in T cells in the brain. Interestingly, increases in CD25 and Bcl-2 were  
39 not observed following IL-10R blockade. Also unlike IL-10R blockade, ICOSL blockade led to an  
40 expansion of both CD8<sup>+</sup> and CD4<sup>+</sup> T cells in the brain, with no expansion of peripheral T cell  
41 populations or neutrophil recruitment to the brain Overall, these results suggest that IL-10 and ICOS  
42 differentially regulate T cell responses in the brain during chronic *T. gondii* infection.

## 43 **Introduction**

44 Immune responses have intricately evolved to protect hosts from a wide range of potentially  
45 harmful pathogens [1, 2], yet these same inflammatory responses can often cause host damage  
46 themselves. The importance of a balanced immune response is apparent in models of infection, where  
47 inflammation is required for pathogen control and survival, yet amplified immune responses observed  
48 after depletion of regulatory T cells or immunosuppressive cytokines often leads to exacerbated tissue  
49 pathology and increased mortality [3-8]. One such immunosuppressive cytokine, IL-10, has been broadly  
50 studied in the context of both tissue homeostasis and during infection, and has been shown to play a key  
51 role in suppressing many aspects of an immune response. Production of IL-10 during immune responses  
52 to infection has been attributed to a wide variety of cell types, including T cells, dendritic cells,  
53 macrophages, NK cells, and B cells [9]. IL-10 also acts on a wide range of cell types, with one of its main  
54 roles being the downregulation of MHC and costimulatory molecules in antigen presenting cells (APCs),  
55 thereby preventing their full activation capacity and limiting T cell responses [10-12]. IL-10 also has  
56 direct effects on T cells, limiting IFN $\gamma$  and IL-2 production, as well as T cell proliferation *in vitro* [13,  
57 14].

58 Infection with the eukaryotic parasite *Toxoplasma gondii* leads to widespread activation of the  
59 immune system and systemic inflammation that is required for host survival [15]. The generation of a  
60 parasite-specific adaptive immune response clears the parasite from most peripheral tissues; however, the  
61 parasite is able to encyst in the central nervous system and establish a chronic infection [16, 17]. This  
62 chronic infection requires ongoing activation and infiltration of highly polarized Th1 cells into the brain  
63 in order to prevent extensive parasite replication and fatal disease [18, 19]. However, like in other models  
64 of infection, regulation of this immune response is also required to promote host survival. In particular,  
65 IL-10 production is required for host survival during acute infection. IL-10 knockout mice succumb to  
66 CD4<sup>+</sup> T cell-mediated immunopathology and excessive inflammatory cytokine production in the  
67 periphery early in the course of infection [3, 20]. Similarly, continued IL-10 production in the chronic

68 phase of infection is also necessary for host survival. IL-10 knockout mice given the antibiotic  
69 sulfadiazine early in the infection to limit parasite replication survive the acute phase of infection, but  
70 later present with similar CD4<sup>+</sup> T cell-mediated fatal immunopathology in the brain [21]. Despite  
71 demonstrating the requirement for IL-10 signaling over the course of *T. gondii* infection, previous studies  
72 have not addressed what additional signals promote immune regulation in the context of chronic  
73 neuroinflammation.

74 ICOS (inducible T cell costimulator) is a costimulatory molecule expressed on activated T cells  
75 [22, 23]. ICOS signaling is important in a wide variety of immune responses, including optimal antibody  
76 class switching and T cell inflammatory cytokine production [23-26]. The primary function attributed to  
77 ICOS is the amplification of effector T cell responses by serving as a costimulatory molecule similar to its  
78 family member CD28 [27]. More recently, ICOS has been shown to also promote immune regulation  
79 through potent induction of IL-10 both *in vitro* and in mouse models of acute inflammation [28-30]. In  
80 addition to promoting production of IL-10, ICOS is also important for maintaining effector regulatory T  
81 cell populations. During homeostasis, blockade of ICOS signaling results in a loss of CD44<sup>hi</sup>CD62L<sup>lo</sup>  
82 effector T<sub>regs</sub> in the spleen [31, 32]. In mouse models of diabetes and helminth infection, a similar loss of  
83 Tregs is seen with a lack of ICOS signaling, in addition to decreased IL-10 production [33, 34]. During  
84 acute *T. gondii* infection, ICOS signaling has been reported to amplify T cell inflammatory responses by  
85 promoting increased IFN $\gamma$  production early in the infection [35, 36]. ICOS appears to play a redundant  
86 role with CD28 in this setting, as mice lacking ICOS are only more susceptible to infection on a CD28<sup>-/-</sup>  
87 background [35]. Together, these reports highlight the context-dependent role of ICOS signaling,  
88 contingent on variables ranging from the type of inflammatory environment to stage of infection [22-36].

89 The role of ICOS, and its relationship to IL-10-mediated regulation of immune responses, in the  
90 context of a chronic neuroinflammatory response to a pathogen is not well understood. In this study, we  
91 first characterized what role IL-10 plays in promoting regulation of immune responses in the chronic  
92 stage of infection by blocking signaling through the IL-10 receptor. This IL-10R blockade during chronic

93 infection led to an expansion of CD4<sup>+</sup> effector T cells correlating with increased expression of CD80 on  
94 APCs, along with widespread immunopathology. Based on previous reports implicating a role for ICOS  
95 in stimulating IL-10 production, we then addressed the question of whether ICOS signaling can promote  
96 suppression of chronic T cell responses in the central nervous system through induction of IL-10.  
97 Surprisingly, we find that blockade of ICOS signaling during chronic infection with *T. gondii* does not  
98 lead to decreased IL-10 production from either regulatory or effector T cells, nor does it lead to impaired  
99 inflammatory cytokine production. In fact, despite maintaining IL-10 levels in the brain, blockade of  
100 ICOSL still results in a loss of T cell regulation, with two to three-fold more effector T cells found in the  
101 inflamed brain. Interestingly, this increase in effector T cells occurred without a loss of T<sub>regs</sub> in the brain  
102 and did not affect parasite burdens. We found this increase in T cell number in the brain to correlate with  
103 increased levels of CD25 and pSTAT5 expression in effector T cells following ICOSL blockade,  
104 suggesting increased responses to IL-2. Along these lines, ICOSL blockade increased T cell proliferation  
105 and expression of the survival factor Bcl-2 among the effector CD4<sup>+</sup> and CD8<sup>+</sup> T cell populations in the  
106 brain. Interestingly, IL-10R blockade did not result in the same increases in IL-2-associated signaling  
107 molecules CD25 and Bcl-2; rather, IL-10R blockade increased the activation state of APCs. Taken  
108 together, our results suggest that ICOS signaling on T cells can suppress STAT5-induced survival signals,  
109 providing a mechanism of local suppression in the context of chronic inflammation in the brain that is  
110 distinct from IL-10-mediated regulation.

## 111 **Materials and Methods**

### 112 ***Mice and infection model***

113 C57Bl/6 and B6.129S6-*Il10<sup>tm1Fhv</sup>/J* (*Tiger*) mice were purchased from Jackson Laboratories. All animals  
114 were kept in UVA specific pathogen-free facilities, and were age and sex matched for all experiments. All  
115 experimental procedures followed the regulations of the Institutional Animal Care and Use Committee at  
116 the University of Virginia. Infections used the avirulent type II *Toxoplasma gondii* strain Me49, which  
117 were maintained in chronically infected Swiss Webster mice (Charles River) and passed through  
118 CBA/J mice (Jackson Laboratories) before experimental infections. For experimental infections, the  
119 brains of chronically infected (4 to 8 weeks) CBA/J mice were homogenized to isolate tissue cysts.  
120 Experimental mice were then injected intraperitoneally with 10 to 20 Me49 cysts.

121

### 122 ***Antibody blockade treatments***

123 For IL-10R blockade studies, chronically infected mice (28-35 days post-infection) were treated  
124 intraperitoneally with 200 µg of a monoclonal antibody blocking the IL-10R (BioXCell) or a control rat  
125 IgG antibody. Treatments were given every 3 days, and mice were euthanized when neurological  
126 symptoms developed between 7-10 days post-antibody treatment. For ICOSL blockade studies,  
127 chronically infected mice (28-35 days post-infection) were treated intraperitoneally with 150 µg of an  $\alpha$ -  
128 ICOSL (CD275) blocking antibody (BioXCell) or a control rat IgG antibody. Antibody treatments were  
129 given every 3 days for 14 days, totaling 5 treatments.

130

### 131 ***Tissue and blood processing***

132 Mice were sacrificed and perfused with 40 mL 1X PBS, and perfused brains, spleens, and lymph nodes  
133 (pooled deep and superficial cervical) were put into cold complete RPMI media (cRPMI) (10% fetal  
134 bovine serum, 1% NEAA, 1% pen/strep, 1% sodium pyruvate, 0.1%  $\beta$ -mercaptoethanol). Brains were  
135 then minced with a razor blade and enzymatically digested with 0.227mg/mL collagenase/dispase and

136 50U/mL DNase (Roche) for 1 hour at 37°C. After enzyme digestion, brain homogenate was passed  
137 through a 70µm filter (Corning). To remove myelin, filtered brain homogenate was resuspended with 20  
138 mL 40% percoll and spun for 25 minutes at 650g. Myelin was then aspirated and the cell pellet was  
139 washed with cRPMI, then resuspended and cells were counted.

140 Spleens and lymph nodes were homogenized and passed through a 40µm filter  
141 (Corning) and pelleted. Lymph node cells were then resuspended in cRPMI and counted. Spleen cells  
142 were resuspended with 2 mL RBC lysis buffer (0.16 M NH<sub>4</sub>Cl). Following RBC lysis, spleen cells were  
143 washed with media and then resuspended with cRPMI for counting.

144 For experiments in which peripheral blood was taken, mice were sacrificed and the right atrium  
145 was cut in preparation for perfusion. Before perfusion, 300µL blood was collected from the chest cavity.  
146 For isolation of circulating leukocytes, collected blood was put in 1mL heparin (100 USP/mL) to prevent  
147 clotting. Samples were then pelleted and resuspended in 2 mL RBC lysis buffer for 2 minutes. Samples  
148 were washed once with cRPMI and a second RBC lysis step was performed. Finally, blood cells were  
149 resuspended in cRPMI for staining and counting. For serum isolation, blood was allowed to clot overnight  
150 at 4°C. Samples were then spun at 14,000 rpm for 10 minutes to separate clotted blood from serum. After  
151 spinning, serum (supernatant) was transferred to a clean tube and stored at -80°C.

152

### 153 ***ELISA***

154 ELISAs for parasite-specific IgG were performed as previously described [37]. Briefly, Immunolon  
155 4HBX ELISA plates (Thermofisher) were coated with 5 µg soluble *Toxoplasma* antigen (STAg)  
156 overnight at 4°C. After antigen coating, plates were washed in 1x PBS with 0.1% Triton and 0.05%  
157 Tween, then blocked with 10% FBS for 2 hours at room temperature. After washing, serial dilutions of  
158 collected serum were added to plate wells overnight at 4°C. After incubation with serum samples, plates  
159 were washed and wells were incubated with HRP (Southern Biotechnology) for 1 hour at room

160 temperature. ABTS peroxidase substrate solution (KBL) was then added to wells and immediately after a  
161 color change plates were read on an Epoch BioTek plate reader using Gen5 2.00 software.

162

### 163 *Flow cytometry*

164 Single cell suspensions from collected tissues were plated in a 96-well plate. Cells were initially  
165 incubated with 50 $\mu$ L Fc block (1 $\mu$ g/mL 2.4G2 Ab (BioXCell), 0.1% rat gamma globulin (Jackson  
166 Immunoresearch)) for 10 minutes at room temperature. Cells were then surface stained for CD3 (145-  
167 2C11), CD19 (eBio1D3), NK1.1 (PK136), ICOS (7E.17G9), ICOSL (HK5.3), MHCII (M5/114.15.2),  
168 CD25 (PC61), CD8 (S3-6.7), CD11c (N418), CD4 (GK1.5), CD80 (16-10A1), CD86 (GL1), CD45 (30-  
169 F11), CD11b (M1/70), Ly6G (1A8), and a live/dead stain for 30 minutes at 4°C. Parasite-specific cells  
170 were identified using a PE-conjugated MHCII tetramer (AVEIHRPVPGTAPPS) (National Institutes of  
171 Health Tetramer Facility). After surface staining, cells were washed with FACS buffer (1% PBS, 0.2%  
172 BSA, and 2mM EDTA) and fixed at 4°C overnight with a fixation/permeabilization kit (eBioscience) or  
173 2% PFA. Following overnight fixation, cells were permeabilized and stained for intracellular markers  
174 Bcl-2 (3F11), Ki67 (SolA15), and Foxp3 (FJK-16S) for 30 minutes at 4°C. Cells were then washed,  
175 resuspended in FACS buffer, and run on a Gallios flow cytometer (Beckman Coulter). Analysis was done  
176 using Flowjo software, v.10.

177

### 178 *Cytokine restimulation*

179 Single cell suspensions were plated into a 96-well plate. For T cell cytokine restimulation, cells were  
180 incubated at 37°C with 20 ng/mL PMA and 1  $\mu$ g/mL ionomycin (Sigma) in the presence of brefeldin A  
181 (Alfa Aesar). After incubation for 5 hours, cell suspensions were washed, surface stained, and fixed.  
182 Cells were then incubated with an antibody against IFN $\gamma$  (XMG1.2) for 30 minutes at 4°C. To  
183 determine IL-10 production, *Tiger* mice expressing eGFP under the IL-10 promoter were used. Cells from  
184 these mice were stimulated with PMA/ionomycin and stained for surface molecules as described above,



185 then lightly fixed with 2% PFA for 30 minutes at room temperature. Cells were then permeabilized with  
186 permeabilization buffer (eBioscience) and incubated with a biotin-conjugated  $\alpha$ -GFP antibody (BD  
187 Biosciences) for 30 minutes at 4°C. Cells were then washed and incubated with a PE-conjugated  
188 streptavidin secondary antibody (eBioscience) for 30 minutes at room temperature. Cells were then fixed  
189 with a fixation/permeabilization kit (eBioscience) overnight at 4°C before other intracellular staining was  
190 performed. For myeloid cell cytokine restimulation, single cell suspensions were plated into a 96-well  
191 plate and incubated with brefeldin A for 5 hours at 37°C before surface and intracellular staining for IL-  
192 12 (C17.8) (eBioscience).

193

#### 194 ***qRT-PCR***

195 Approximately 100 mg brain tissue was put into 1 mL Trizol (Ambion) in bead beating tubes (Sarstedt)  
196 containing 1mm zirconia/silica beads (BioSpec). Using a Mini-bead beater (Biospec), tissue was  
197 homogenized for 30 seconds and RNA extraction was completed using the manufacturer's instructions  
198 (Ambion). For cDNA synthesis, a High Capacity Reverse Transcription Kit (Applied Biosystems) was  
199 used. qRT-PCR was set up using a 2X Taq-based mastermix (Bioline) and Taqman gene expression  
200 assays (Applied Biosystems) and reactions were run on a CFX384 Real-Time System (Bio-Rad). HPRT  
201 was used as a housekeeping gene for all reactions and relative expression compared to control treated  
202 animals was calculated as  $2^{(-\Delta\Delta CT)}$ .

203

#### 204 ***T. gondii* cyst counts**

205 After mincing with a razor blade, brain tissue was passed through an 18- and 22-gauge needle. 30 $\mu$ L of  
206 brain homogenate was then placed onto a microscope slide (VWR) and cysts were counted manually on a  
207 brightfield DM 2000 LED microscope (Leica).

208

#### 209 ***Immunohistochemistry***

210 Brains from mice were embedded in OCT and flash frozen on dry ice. Samples were then stored at -20°C  
211 until cutting. For Ki67 immunofluorescence staining, fresh frozen sections were lightly fixed in 25%  
212 EtOH/75% acetone solution for 15 minutes at -20°C. Sections were then blocked in 1% PBS containing  
213 2% goat serum (Jackson Immunoresearch), 0.1% triton, and 0.05% Tween 20 for 1 hour at room  
214 temperature, then incubated with primary antibodies at 4°C overnight. After primary staining, sections  
215 were washed with 1% PBS and incubated with secondary antibodies for 30 minutes at room temperature.  
216 Finally, sections were nuclear stained with DAPI (Thermo Scientific) for 5 minutes at room temperature.  
217 Sections were then covered with aquamount (Lerner Laboratories) and coverslips (Fisherbrand).

218 For pSTAT5 immunofluorescence staining, fresh frozen sections were fixed in 3.2% PFA for 20  
219 minutes at room temperature and then permeabilized with ice cold 90% methanol for 10 minutes at -20°C  
220 [31]. Sections were then incubated with blocking buffer and an anti-pSTAT5 (D47E7) (Cell Signaling  
221 Technologies) primary antibody as described above. After primary antibody staining, pSTAT5 signal was  
222 amplified using an anti-rabbit biotinylated antibody (Jackson Immunoresearch) before using a  
223 streptavidin secondary antibody. All images were captured using a DMI6000 B widefield microscope  
224 with a Hamamatsu C10600 Orca R<sup>2</sup> digital camera (Leica), and visualized using Metamorph software.  
225 Images were then analyzed using Image J software.

226 For quantification of the number of Ki67- or pSTAT5-expressing cells, 12-15 equal-sized  
227 pictures were taken (40x) within each brain slice, and the numbers of Ki67+ or pSTAT5+ CD4+ or CD8+  
228 cells were counted in each image. Numbers from each picture were then averaged and reported as the  
229 average number of Ki67+ or pSTAT5+ per 100µm<sup>2</sup> or 500µm<sup>2</sup> per mouse, respectively.

230

### 231 ***Statistics***

232 Statistical analysis comparing two different groups at a single time point was performed in Prism software  
233 (v. 7.0a) using a Student's t test. In some cases, multiple experiments from different infection dates were  
234 combined to show natural biological variation between infections. When data from multiple experiments

235 were combined, a randomized block ANOVA was used in R v.3.4.4 statistical software. This statistical  
236 test accounted for natural variability between experimental dates by modeling the treatment (IgG vs.  $\alpha$ -IL-  
237 10R or  $\alpha$ -ICOSL) as a fixed effect and the experimental date as a random effect. The particular test used  
238 for each individual panel shown is specified in the figure legend. P values are displayed as follows: ns=  
239 not significant, \*  $p < 0.05$ , \*\*  $p < 0.01$ , \*\*\*  $p < 0.001$ . All data were graphed using Prism software, and the  
240 number of mice per group is indicated in the figure legend.

241 **Results**

242 *Blockade of IL-10R during chronic T. gondii infection leads to broad changes in the immune response*  
243 *and results in fatal immunopathology in brain.*

244 During chronic infection with *T. gondii*, both effector T cells and T<sub>regs</sub> recruited to the brain are  
245 capable of producing IL-10 [38]. Previously published results have shown a requirement for IL-10  
246 signaling to limit fatal immunopathology in both the acute and chronic stages of infection [3, 21, 39, 40].  
247 Despite the necessity for IL-10 over the course of infection with *T. gondii*, previous studies addressing the  
248 role of IL-10 in the chronic phase of infection relied on total IL-10 knockout mice, which succumb to  
249 fatal immunopathology during the first two weeks of infection [41]. In order for these mice to survive to  
250 the chronic stage of infection, the anti-parasitic drug sulfadiazine must be administered for the first two  
251 weeks of infection in order to limit parasite replication and dissemination. These previously published  
252 studies reported that, after sulfadiazine treatment, IL-10 knockout mice subsequently presented with  
253 CD4<sup>+</sup> T cell dependent lethal immunopathology and died late in the chronic stage of disease [21]. It is  
254 still unknown, however, how a loss of IL-10 only in the chronic phase of infection influences immune  
255 responses. Thus, we treated mice with an  $\alpha$ -IL-10R blocking antibody beginning four weeks post  
256 infection. Mice treated with an  $\alpha$ -IL-10R blocking antibody during the chronic stage of infection  
257 presented with overt disease and became moribund between 7 to 10 days post-treatment. H&E staining of  
258 tissue sections from brains of  $\alpha$ -IL-10R-treated mice showed increased leukocyte infiltration and  
259 associated areas of necrosis not seen in control treated animals (Figure 1A-B). The increased numbers of  
260 immune cells in the brains of  $\alpha$ -IL-10R-treated mice included increases in both CD4<sup>+</sup>Foxp3<sup>-</sup> T cells and  
261 infiltrating macrophages (Figure 1C and Supplementary Figure 1A). Though the increase in T cell  
262 number in the brains of  $\alpha$ -IL-10R-treated mice predominantly came from an increase in the CD4<sup>+</sup>Foxp3<sup>-</sup>  
263 T cell compartment and not the CD8<sup>+</sup> T cell compartment, an increased frequency of both Ki67<sup>+</sup> CD4<sup>+</sup>  
264 and CD8<sup>+</sup> effector T cells was observed (Figure 1D). Interestingly, using an MHCII tetramer reagent to  
265 measure CD4<sup>+</sup> T cells specific for the parasite, we observed no significant increase in the number of

266 tetramer-positive CD4<sup>+</sup>Foxp3<sup>-</sup> T cells (Figure 1E). Though this analysis of antigen specificity was done  
267 using only a single parasite peptide, this result suggests that IL-10R blockade in the chronic phase of  
268 infection leads to the expansion of CD4<sup>+</sup> effector T cells with potentially different antigen specificities,  
269 possibly through the expansion of other parasite-specific T cell clones or self-antigen-specific T cell  
270 clones.

271 The increased proliferation of effector T cells in the brain correlated with an increase in the  
272 expression of costimulatory molecule CD80 on infiltrating dendritic cells and macrophages in  $\alpha$ -IL-10R-  
273 treated mice (Figure 1F). The increased numbers of immune cells infiltrating the brain was associated  
274 with increased mRNA levels of many pro-inflammatory cytokines and chemokines, including IFN $\gamma$ , IL-6,  
275 TNF $\alpha$ , IL-17, and CXCL1, demonstrating a widespread increase in inflammation in the brain in the  
276 absence of IL-10 signaling (Figure 1G-H). An increase in IL-17 production is notable in this model, as  
277 infection of wild-type mice with *T. gondii* typically leads to a robust Th1-polarized immune response,  
278 characterized by IL-12 and IFN $\gamma$  production that persists throughout the chronic stage, with very little  
279 production of Th17-associated cytokines [42, 43]. Indeed, production of IL-17 has been linked to a loss of  
280 IL-27-mediated regulation of immune responses during infection with *T. gondii* [43, 44], suggesting a  
281 pathogenic role for IL-17 in this context.

282 Production of IL-17 and CXCL1 has previously been shown to enhance recruitment of  
283 neutrophils to inflamed tissues and enhance their activity in certain disease contexts [45-50]. Neutrophil  
284 recruitment to the central nervous system however, has been shown to be detrimental in many cases [50-  
285 52]. With the increased mRNA levels of both IL-17 and CXCL1 seen in the brain after IL-10R blockade,  
286 we wanted to assess whether more neutrophils were recruited to the inflamed brain in this context. Indeed,  
287  $\alpha$ -IL-10R-treated mice had a nearly three-fold increase in neutrophil numbers in the brain in comparison  
288 to control-treated mice (Figure 1I-J and Supplementary Figure 1B-C). Despite the increased T cell  
289 response in the brain with IL-10R blockade, no change in the number of parasite cysts was observed  
290 (Figure 1K).

291 The effects of IL-10R blockade during the chronic phase of infection were not limited to the  
292 inflamed brain, as increased CD4<sup>+</sup>Foxp3<sup>-</sup> effector T cells and myeloid cells were found in the spleens of  
293  $\alpha$ -IL-10R-treated mice (Supplementary Figure 1D-E). Myeloid cells in the spleen were also highly  
294 activated, with higher levels of CD80 expression on APCs in the spleens of  $\alpha$ -IL-10R-treated mice as  
295 opposed to controls (Supplementary Figure 1F). Large areas of necrosis were also observed in the livers  
296 of  $\alpha$ -IL-10R-treated mice (Supplementary Figure 1G-H), suggesting that the increased inflammatory  
297 response seen following IL-10R blockade can contribute to extensive immunopathology in not only the  
298 brain but peripheral tissues as well. Overall, a loss of IL-10 signaling specifically during the chronic  
299 infection led to widespread immune cell activation that rapidly resulted in fatal immunopathology.

300

301 *Blockade of ICOSL does not affect IL-10 production during chronic infection, but leads to expanded T*  
302 *cell populations in the brain.*

303 Despite clear evidence that IL-10-mediated regulation of immune responses during *T. gondii*  
304 infection is required for host survival, little is known about what signals can induce IL-10 production in  
305 activated T cells during the chronic inflammation in the brain associated with the later stages of infection.  
306 Several studies have implicated a role for ICOS in inducing IL-10 production in cases of acute  
307 inflammation [29, 33]. We found ICOS-expressing T cells in the brain during chronic *T. gondii* infection,  
308 as well as infiltrating APCs expressing the ICOS-ligand (ICOSL) (Figure 2A-B). To address whether  
309 ICOS signaling is important for T cell production of IL-10 in the brain during chronic infection, we  
310 treated chronically infected IL-10-eGFP reporter (*Tiger*) mice with the ICOSL blocking antibody.  
311 Surprisingly, following ICOSL blockade in the chronic stage of infection, we did not see decreases in IL-  
312 10 production from either CD4<sup>+</sup>Foxp3<sup>-</sup> effector T cells or CD4<sup>+</sup>Foxp3<sup>+</sup> regulatory T cells in the brain  
313 (Figure 2C), and IL-10 mRNA expression from whole brain homogenate was also not decreased (Figure  
314 2D). Although levels of IL-10 were not affected after  $\alpha$ -ICOSL treatment, we unexpectedly observed a  
315 two- to three-fold increase of both CD4<sup>+</sup>Foxp3<sup>-</sup> and CD8<sup>+</sup> effector T cells, respectively (Figure 2E). This

316 increase in effector T cell number was not due to a loss of the local regulatory T cell population, as their  
317 numbers in the brain were also increased, though to a lesser degree than the effector T cell populations  
318 (Figure 2E). Infiltrating myeloid cell numbers were also assessed, revealing almost a two-fold increase in  
319 dendritic cells in the brain compared to control treated animals (Supplementary Figure 2A). Though  
320 increased numbers of dendritic cells were found in the brain following  $\alpha$ -ICOSL treatment, there was no  
321 effect on IL-12 production from either the dendritic cells or macrophages isolated from the brain  
322 (Supplementary Figure 2B-C), suggesting that continued production of IL-12 is not reliant on ICOS-  
323 ICOSL interactions. We also found an increase in the number of IFN $\gamma$ -producing effector T cells in the  
324 brain, while mRNA levels of other pro-inflammatory cytokines and chemokines were not increased  
325 (Supplementary Figure 2D-E). The increased numbers of T cells in the brains  $\alpha$ -ICOSL-treated animals  
326 could be seen dispersed throughout the brain parenchyma (Figure 2F-G), though unlike  $\alpha$ -IL-10R treated  
327 animals, ICOSL blockade was not lethal in the observed timeframe. Additionally, we observed an  
328 increase in the number of tetramer-positive CD4<sup>+</sup> effector T cells in the brain (Figure 2H), suggesting  
329 that ICOSL blockade can lead to an expansion of parasite-specific CD4<sup>+</sup> effector T cells in the brain.  
330 Another distinction between IL-10R blockade and ICOSL blockade in the chronic phase of infection was  
331 a difference in neutrophil recruitment. Whereas an increase in neutrophil numbers in the brain was seen in  
332  $\alpha$ -IL-10R-treated mice (Figure 1), no significant increase was seen in  $\alpha$ -ICOSL-treated mice (Figure 2I-J).

333         Blockade of ICOSL primarily affected the T cell populations in the CNS and did not affect T cell  
334 numbers in the spleen, draining LNs, or blood of  $\alpha$ -ICOSL-treated mice (Supplementary Figure 2F-H).  
335 ICOS signaling has also been shown to be crucial for primary antibody responses to infection [26, 53,  
336 54]. In order to assess whether the increased T cell numbers found in the brains of  $\alpha$ -ICOSL treated  
337 animals was merely a result of a change in parasite burden due to decreased antibody production, both  
338 parasite-specific serum IgG titers and brain cyst burden was measured. No change was seen in either  
339 circulating parasite-specific IgG (Supplementary Figure 2I) or parasite burden in the brain (Figure 2K).

340 Together, these results suggest that ICOS signaling limits excessive T cell responses in the brain during  
341 chronic neuroinflammation independent of changes in either IL-10 production or parasite burden.

342

343 *ICOSL blockade during chronic infection is associated with increases in Ki67- and Bcl-2-expressing*  
344 *effector T cells in the brain.*

345 We next wanted to determine how lack of ICOS-ICOSL interaction during chronic inflammation  
346 leads to increased numbers of T cells in the CNS. Using immunofluorescence staining for Ki67, increased  
347 numbers of proliferating CD4+ and CD8+ effector T cells were found throughout the brain after ICOSL  
348 blockade during chronic infection (Figure 3A-D). Using flow cytometry, we confirmed this increase in  
349 the number of proliferating effector T cells in the brain (Figure 3E). Distinct from IL-10R blockade, the  
350 increase in Ki67+ effector T cells in the brain following ICOSL blockade was not correlated with an  
351 increase in CD80 or CD86 expression on infiltrating APCs (Figure 3F). Rather, ICOSL blockade led to  
352 the upregulation of the pro-survival factor Bcl-2 in both CD4+Foxp3- and CD8+ effector T cells isolated  
353 from the brain (Figure 3G-I). The above results suggest that ICOS limits effector T cell proliferation and  
354 survival factor expression during chronic neuroinflammation

355

356 *Blockade of ICOSL increases CD25 expression and STAT5 phosphorylation in effector T cells in the*  
357 *brain during chronic infection.*

358 IL-2 signaling in T cells has been shown to support both their proliferation and survival [55, 56].  
359 Thus, we wanted to determine if the increased effector T cell proliferation and survival factor Bcl-2  
360 expression could be a result of increased response to IL-2 following ICOSL blockade. After ICOSL  
361 blockade, both CD4+Foxp3- and CD8+ effector T cells isolated from the brain expressed higher levels of  
362 CD25, and there was a two- to three-fold increase in the total number of CD25+ effector T cells in the  
363 brain compared to control treated animals (Figure 4A-D). In order to assess whether more of the  
364 infiltrating T cells in the brain may be responding to IL-2, we used immunofluorescence staining for



365 phosphorylated STAT5 (pSTAT5), the main signaling molecule downstream of the IL-2R. Correlated  
366 with the increased number of CD25<sup>+</sup> effector T cells found in the brain with ICOSL blockade, we  
367 observed increased numbers of pSTAT5-positive CD4<sup>+</sup> and CD8<sup>+</sup> T cells in the brains of  $\alpha$ -ICOSL-  
368 treated animals (Figure 4E-J). Taken together, these data suggest that after ICOSL blockade, effector T  
369 cells may maintain higher levels of CD25 and pSTAT5, which in turn could support increased  
370 proliferation and Bcl-2 expression.

371

372 *IL-10R blockade does not affect Bcl-2 or CD25 expression on T cells in the brain during chronic*  
373 *infection.*

374 While increased expression of both Bcl-2 and CD25 was seen on effector T cells in the brain  
375 following ICOSL blockade, no change in Bcl-2 expression was seen in effector T cell populations  
376 isolated from the brains of  $\alpha$ -IL-10R-treated mice (Figure 5A-B). Additionally, increased levels of CD25  
377 were not observed to the same degree with  $\alpha$ -IL-10R treatment, as there were no changes in the levels of  
378 CD25 expression on CD4<sup>+</sup>Foxp3<sup>-</sup> T cells, and only a slight increase in CD25 expression on the CD8<sup>+</sup> T  
379 cell population (Figure 5C). Overall, though both IL-10R blockade and ICOSL blockade resulted in  
380 increased numbers of effector T cells in the brain, IL-10R blockade correlated with increased APC  
381 activation and inflammatory cytokine mRNA expression, while ICOSL blockade correlated with  
382 upregulation of IL-2-associated signaling molecules in effector T cells. These data further support that  
383 ICOS and IL-10 signaling pathways can differentially promote regulation of effector T cell responses in  
384 the brain during chronic infection.

## 385 **Discussion**

386 Inflammation is required to promote clearance of pathogens, but preventing excessive  
387 inflammation during immune responses to infection is necessary to avoid immune-mediated tissue  
388 damage [3, 15, 57]. In cases of chronic infection, this balance between inflammation and regulation must  
389 be maintained over long periods of time [21, 43], but many of the signals required to maintain control of  
390 ongoing immune responses are not well understood. Our results identify one such signal, ICOS, whose  
391 expression on activated T cells in the chronically infected brain provides a suppressive signal preventing  
392 overabundant T cell accumulation in the inflamed CNS. We show that ICOSL blockade is associated with  
393 increased expression of IL-2-associated signaling molecules CD25, pSTAT5, and Bcl-2, as well as  
394 effector T cell accumulation in the brain.

395 ICOS, similar to its family member CD28, was initially characterized for its ability to amplify  
396 both B cell antibody production and T cell inflammatory cytokine production in cases of acute  
397 inflammation [24, 25, 53]. The pro-inflammatory role for ICOS signaling was subsequently supported by  
398 human data, as humans carrying mutations in the ICOS gene are included in the class of mutations known  
399 as common variable immunodeficiency (CVID) [58-60]. Patients with CVID have increased susceptibility  
400 to bacterial infections, and are diagnosed based on severely decreased class-switched antibody  
401 production, further implicating ICOS as important for T cell-dependent B cell responses [59].  
402 Interestingly, further data from patients with CVID began to emerge highlighting widespread immune  
403 system abnormalities outside of the B cell compartment, particularly splenomegaly, a loss of naïve CD4+  
404 T cells and expansion of activated CD4+ T cells, and increased T cell inflammatory cytokine production  
405 [58, 61, 62]. Additionally, despite being defined as an immunodeficiency disease, about 20% of CVID  
406 patients also present with autoimmune complications, though the pathogenesis of this autoimmunity  
407 remains unclear [63].

408 Studies regarding the role of ICOS in promoting regulation of immune responses largely come  
409 from mouse models, where ICOS has been shown to both support T<sub>reg</sub> populations and promote IL-10

410 production [29, 31, 33, 34]. Surprisingly, we found no evidence of a local T<sub>reg</sub> defect following ICOSL  
411 blockade, suggesting that T<sub>regs</sub> in the brain during chronic infection rely on signals other than ICOS to  
412 support their survival and accumulation in the tissue, as well as their production of IL-10. Many activated  
413 effector T cells in the brain continue to produce IL-2 in the chronic phase of infection with *T. gondii*, so it  
414 is possible that the largely CD25<sup>+</sup> T<sub>regs</sub> in the CNS rely mainly on IL-2 signals for their maintenance in an  
415 inflamed tissue, whereas other signals are required during homeostasis when lower levels of IL-2 would  
416 be present in the absence of an ongoing effector T cell response

417         One of the main differences observed between IL-10R blockade and ICOSL blockade in the  
418 chronic phase of infection was the disparity in the magnitude of response. IL-10R is expressed more  
419 broadly than ICOS, which may explain the widespread inflammation and lethality of IL-10R versus  
420 ICOSL blockade. IL-10R is expressed by most hematopoietic cells, but can also be induced on non-  
421 hematopoietic cells such as fibroblasts and endothelial cells, rendering them also able to respond to IL-10  
422 in inflammatory settings [64-66]. In the context of chronic *T. gondii* infection, this could explain why  
423 changes were seen in myeloid and T cell subsets in both the brain and peripheral tissues following  $\alpha$ -IL-  
424 10R blockade. On the other hand, ICOS is only expressed on activated T cells during chronic *T. gondii*  
425 infection, and its highest levels of expression were found in the inflamed brain. This more limited  
426 expression pattern of ICOS compared to IL-10R could potentially explain the more local and specific  
427 response to ICOSL blockade.

428         Another interesting aspect of the immunological phenotype seen with IL-10R blockade during  
429 chronic infection was the differential effects on the accumulation of CD8<sup>+</sup> and CD4<sup>+</sup> effector T cell  
430 populations in the brain. Following IL-10R blockade, local APCs in the brain upregulate CD80, so it is  
431 possible that the CD4<sup>+</sup> effector T cells infiltrating the brain are interacting with the highly activated local  
432 MHCII<sup>+</sup> APCs more so than the CD8<sup>+</sup> effector T cells, leading to their increased accumulation. It is  
433 interesting to note that, of the brain-infiltrating APCs isolated during chronic *T. gondii* infection, only a  
434 small fraction of them are classic CD8 $\alpha$ <sup>+</sup> cross-presenting DCs that could interact in a TCR-dependent

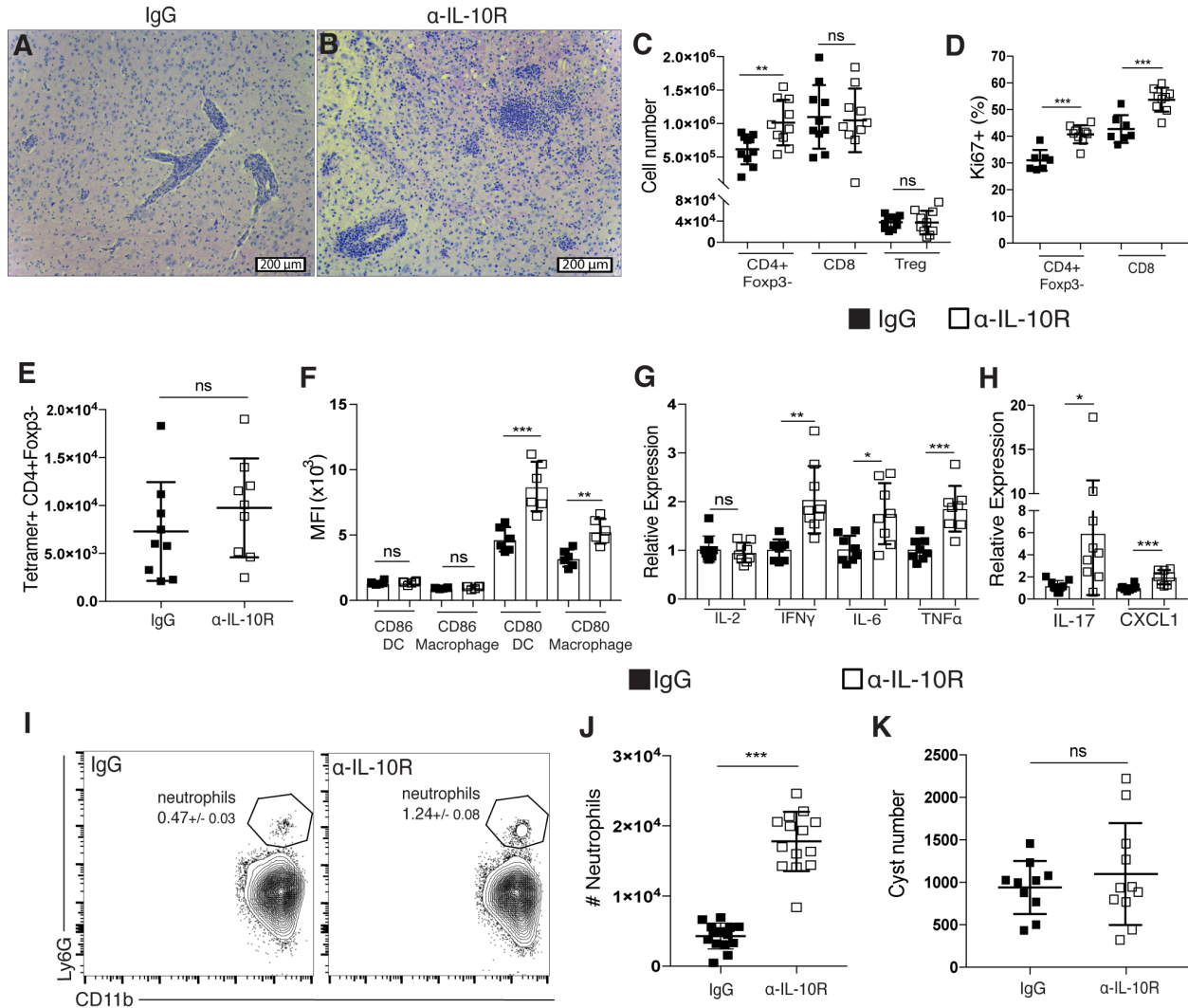
435 fashion with infiltrating CD8+ T cells [67]. This could suggest that the activated CD8+ effector T cells in  
436 the brain rely less on local restimulation through TCR-MHC and costimulatory interactions, and are  
437 therefore less affected by extrinsic mechanisms of suppression through APCs in this context. Overall, it is  
438 largely unknown what kinds of secondary signals, such as TCR-MHC or costimulatory interaction, are  
439 required for activated T cells to carry out effector function and survive at a distal site of inflammation  
440 after initial priming in secondary lymphoid organs, though it is likely these requirements differ in some  
441 way for CD8+ and CD4+ T cells. Though the overall number of CD8+ effector T cells in the brain is not  
442 increased, we still observed an increased frequency of Ki67+ CD8+ T cells in the brain after IL-10R  
443 blockade, suggesting that this population is still responsive to IL-10-mediated suppression; perhaps  
444 through an intrinsic response to IL-10 that limits their proliferative capacity. IL-10 has been shown to be  
445 able to directly inhibit proliferation of CD8+ T cells *in vitro* [14], as well as control the threshold of their  
446 response to antigen upon initial activation [68]. Much is still unknown about the direct effects of IL-10 on  
447 activated CD8+ T cells that could contribute to their regulation, though these data further suggest that  
448 CD8+ effector T cells may be differentially regulated from the CD4+ effector T cell compartment in the  
449 brain.

450 Two well-characterized inhibitory co-receptors are CTLA-4 and PD-1, both of which have been  
451 shown to carry out their inhibitory effect at least partially through inhibition of the PI3K/Akt signaling  
452 pathway [69, 70]. In this light, it is interesting to consider ICOS, which is a potent activator of the  
453 PI3K/Akt pathway [71, 72], as also providing an inhibitory signal to T cells during chronic inflammation.  
454 Initial Akt activation induced during priming has been associated with increased T cell responses, both  
455 through promotion of T cell proliferation and survival [73-75]. However, more recent reports have shown  
456 that constitutive Akt activation in CD8+ T cells is associated with decreased expression of CD122 and  
457 Bcl-2, and can promote the development of short-lived effector T cells over the development of memory  
458 T cells, while constitutive STAT5 signaling can maintain Bcl-2 expression and favor the development of  
459 memory precursor cells [76, 77]. These results emphasize that the fate of T cells is extremely sensitive to

460 both the level and duration of signaling cascades like PI3K/Akt. During the chronic neuroinflammation  
461 seen with *T. gondii* infection, continued activation of Akt downstream of ICOS in activated T cells in the  
462 brain could potentially serve as an intrinsic mechanism of controlling T cell responses by downregulating  
463 IL-2-associated signaling molecules and driving effector T cells in the brain to be short-lived effectors  
464 rather than memory precursors.

465 Overall, we provide evidence that ICOS costimulation provides an inhibitory signal to antigen-  
466 experienced effector T cells in the chronically inflamed brain. These data postulate a regulatory role for  
467 ICOS in T cells during chronic neuroinflammation that is distinct and more specific than the suppressive  
468 role of IL-10. Altogether, while we show that IL-10 is absolutely required for preventing exaggerated  
469 immune responses and immunopathology, other regulatory signals like ICOS are also likely at play  
470 during chronic inflammation that provide more fine-tuned suppression of ongoing immune responses  
471 without affecting IL-10-mediated suppression.

472 **Figures**



473

474 **Figure 1. Blockade of IL-10R during chronic *T. gondii* infection leads to broad changes in**

475 **the immune response and fatal immunopathology in the brain. (A-K) Rat IgG or an  $\alpha$ -IL-**

476 **10R blocking antibody was administered to chronically infected mice beginning at day 28 post-**

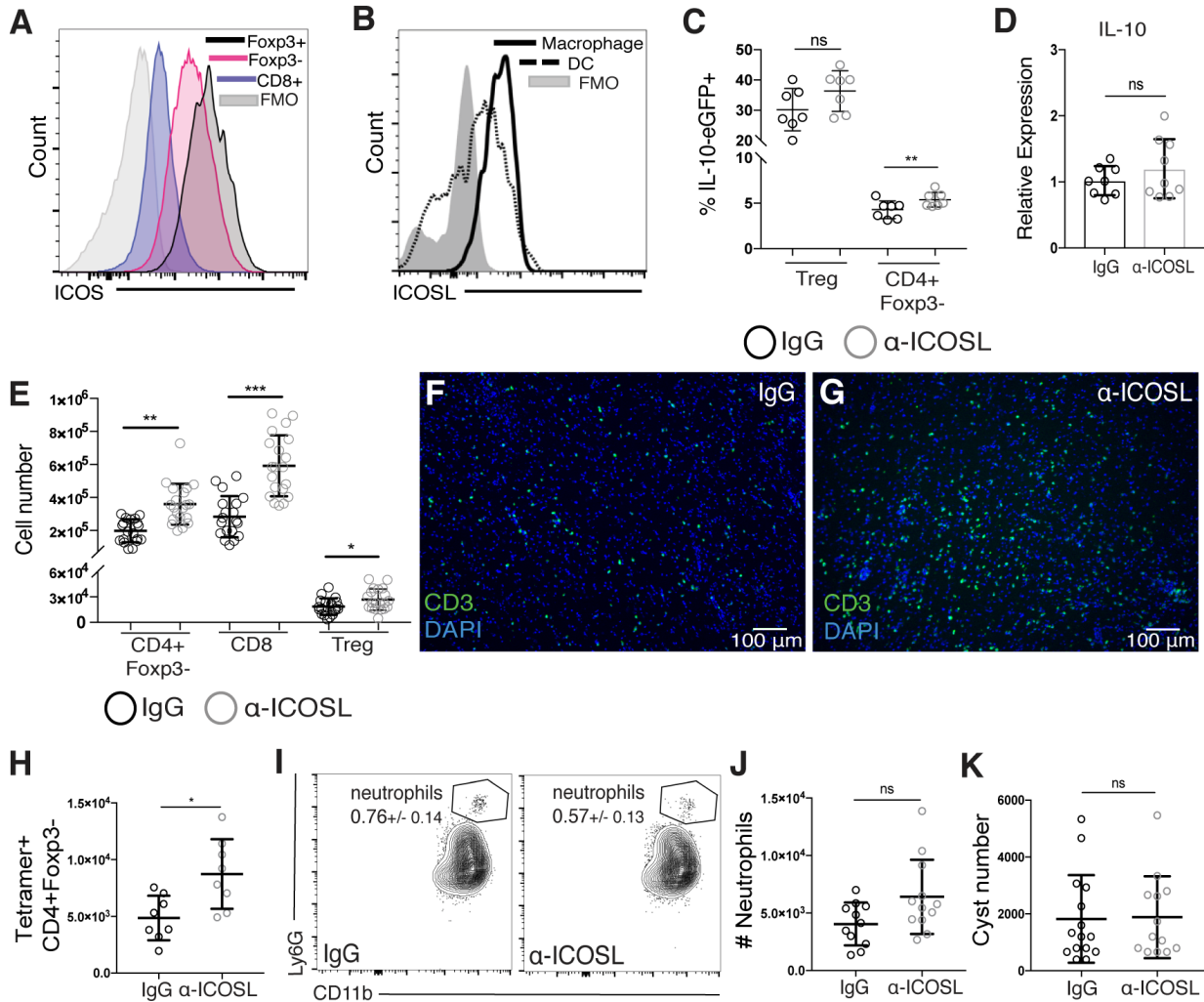
477 **infection. (A-B) Representative H&E stained brain sections from a chronically infected control-**

478 **treated mouse (A) and an  $\alpha$ -IL-10R-treated mouse (B). (C) T cells isolated from the brain were**

479 **analyzed by flow cytometry. Effector CD4+ T cells (CD4+Foxp3-), CD8 T cells, and T<sub>regs</sub>**

480 **(CD4+Foxp3+) were enumerated (n=5 per group, data is pooled from two independent**

481 experiments and analyzed using a randomized block ANOVA). **(D)** The frequency of Ki67+  
482 effector T cells was measured by flow cytometry from mononuclear cells isolated from the  
483 brains of control and  $\alpha$ -IL-10R-treated mice (n=3-5 per group, data is pooled from two  
484 independent experiments and analyzed using randomized block ANOVA). **(E)** Parasite-specific  
485 CD4+ effector T cells were assessed by flow cytometry using an MHCII-peptide tetramer. **(F)**  
486 The mean fluorescence intensity (MFI) of CD80 and CD86 on brain-infiltrating APCs. DCs were  
487 gated on CD45<sup>hi</sup>CD3<sup>-</sup>NK1.1<sup>-</sup>CD19<sup>-</sup>CD11c<sup>+</sup>MHCII<sup>hi</sup> live singlet cells and macrophages were  
488 gated on CD45<sup>hi</sup>CD3<sup>-</sup>NK1.1<sup>-</sup>CD19<sup>-</sup>CD11c<sup>-</sup>CD11b<sup>+</sup> live singlet cells (n=6 per group, data is  
489 representative of 3 independent experiments and analyzed using Student's t test). **(G-H)** qRT-  
490 PCR was done using mRNA isolated from whole brains of chronically infected control or  $\alpha$ -IL-  
491 10R-treated mice. Relative expression was normalized to the control (IgG-treated) group (n=4-5  
492 per group, data is pooled from two independent experiments and analyzed using randomized  
493 block ANOVA). **(I)** Representative flow plots showing the neutrophil population isolated from  
494 the brains of chronically infected mice. Neutrophils were gated on CD45<sup>hi</sup>CD3<sup>-</sup>CD19<sup>-</sup>NK1.1<sup>-</sup>  
495 CD11b<sup>+</sup>Ly6G<sup>+</sup> live singlet cells. Number in plot indicates the mean frequency +/- standard error.  
496 **(J)** Neutrophils were identified by flow cytometry from cells isolated from the brains of  
497 chronically infected control or  $\alpha$ -IL-10R-treated mice (n=4-5 per group, data is pooled from  
498 three independent experiments and analyzed by randomized block ANOVA). **(K)** Total cyst  
499 numbers from the brains of chronically infected control and  $\alpha$ -IL-10R-treated mice were counted  
500 using light microscopy (n=3-4 per group, data is pooled from three independent experiments and  
501 analyzed by randomized block ANOVA). \* denotes p<0.05, \*\* denotes p<0.01, and \*\*\* denotes  
502 p<0.001 for all panels.



503

504 **Figure 2. Blockade of ICOSL does not affect IL-10 production during chronic *T. gondii***

505 **infection, but leads to expanded T cell populations in the brain. (A) ICOS expression on T**

506 **cells and (B) ICOSL expression on infiltrating myeloid cells isolated from the brains of**

507 **chronically infected mice using flow cytometry. Immune cell populations were gated as**

508 **described above. (C) Chronically infected IL-10-eGFP reporter (*Tiger*) mice were treated with**

509 **an  $\alpha$ -ICOSL blocking antibody beginning 4 weeks post-infection. Blocking or control antibody**

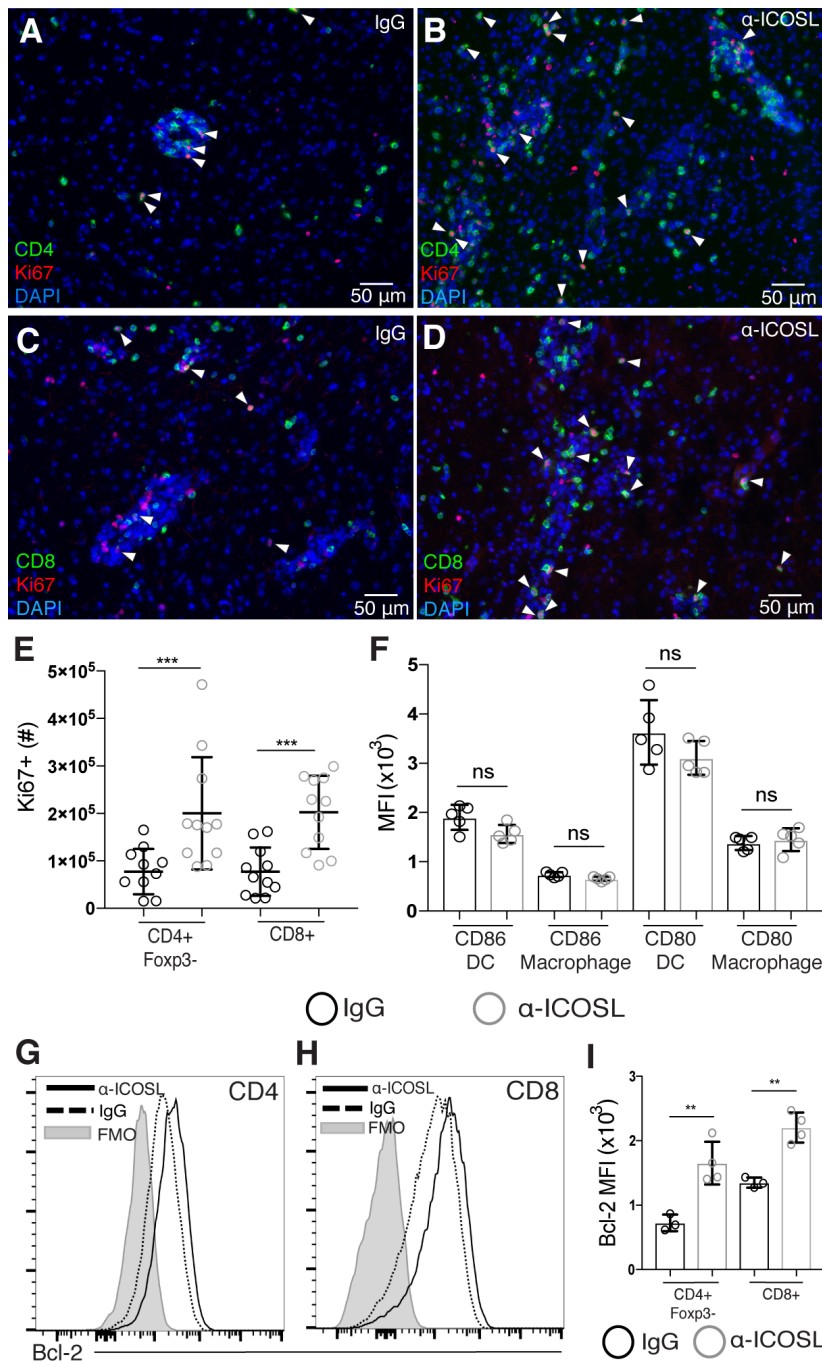
510 **was given every 3 days for 2 weeks. The frequency of IL-10-GFP+ CD4 effector and T<sub>reg</sub> cells**

511 **isolated from the brain is shown (n=3-4 per group, data is pooled from two independent**

512 **experiments and analyzed using randomized block ANOVA). (D) The relative expression of IL-**



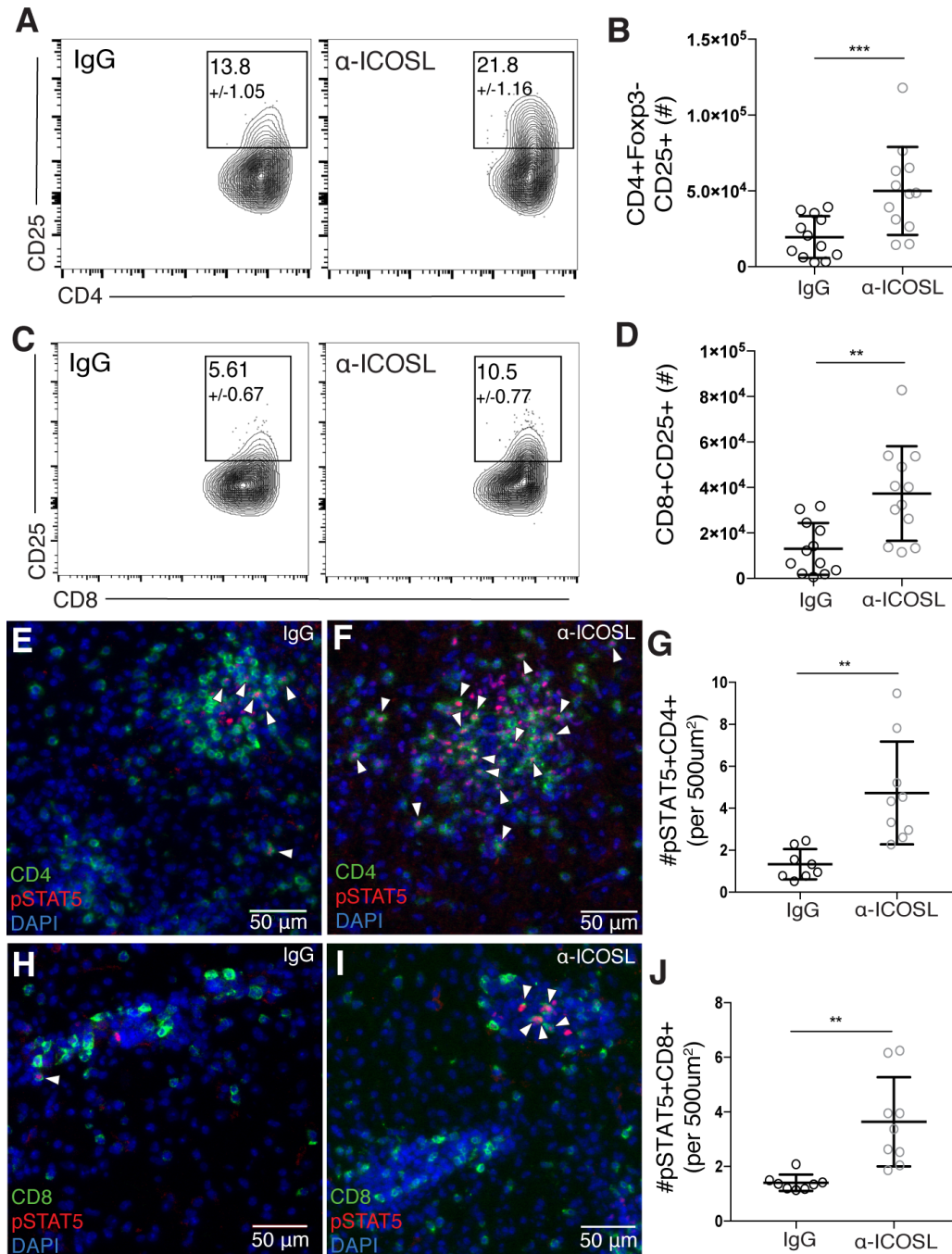
513 10 mRNA in chronically infected whole brains treated with control or  $\alpha$ -ICOSL blocking  
514 antibody. Relative expression was normalized to the control (IgG-treated) group (n=4 per group,  
515 data is pooled from two independent experiments and analyzed using randomized block  
516 ANOVA). **(E-K)** Chronically infected WT mice were treated with an  $\alpha$ -ICOSL blocking  
517 antibody or control rat IgG. **(E)** Total T cell numbers isolated from the brain were analyzed by  
518 flow cytometry (n=3-4 per group, representative data is pooled from 5 independent experiments  
519 and analyzed by randomized block ANOVA). **(F-G)** Representative brain sections stained for  
520 CD3 (green) from control **(F)** or  $\alpha$ -ICOSL-treated **(G)** mice. **(H)** Parasite-specific CD4<sup>+</sup> effector  
521 T cells were assessed by flow cytometry using an MHCII-peptide tetramer. **(I)** Representative  
522 flow plots of the neutrophil population and **(J)** total numbers of neutrophils isolated from the  
523 brain. Number in plots indicates the mean frequency +/- standard error. (n=3-4 per group, data is  
524 pooled from three independent experiments and analyzed using randomized block ANOVA). **(K)**  
525 Total cyst numbers from the brains of chronically infected control and  $\alpha$ -ICOSL-treated mice  
526 enumerated by light microscopy (n=4-5 per group, data is pooled from three independent  
527 experiments and analyzed using randomized block ANOVA). \* denotes p<0.05, \*\* denotes  
528 p<0.01, and \*\*\* denotes p<0.001 for all panels.



529  
530

531 **Figure 3. ICOSL blockade during chronic infection is associated with increases in Ki67-**  
532 **and Bcl-2-expressing effector T cells in the brain. (A-D)** Brain sections from chronically  
533 **infected control (A, C) and  $\alpha$ -ICOSL-treated (B, D) mice were stained for CD4 or CD8 (green),**  
534 **Ki67 (red), and DAPI (blue). White arrowheads indicate Ki67+ CD4 or CD8 T cells. (E) The**

535 number of Ki67+ effector T cells in the brains of control or  $\alpha$ -ICOSL-treated mice was analyzed  
536 by flow cytometry (n=3-4 mice per group, data is pooled from 3 independent experiments and  
537 analyzed by randomized block ANOVA). **(F)** The MFI of CD80 and CD86 on infiltrating APCs  
538 isolated from the brain after  $\alpha$ -ICOSL or control treatment (n=5 mice per group, data is  
539 representative of 3 independent experiments and analyzed using Student's t test). **(G-H)**  
540 Representative histograms of Bcl-2 expression measured by flow cytometry on effector CD4+  
541 **(G)** and effector CD8+ **(H)** T cells isolated from the brain. **(I)** The MFI of Bcl-2 on effector T  
542 cell populations isolated from the brains of chronically infected control or  $\alpha$ -ICOSL-treated mice  
543 (n=3-4 per group, data is representative of 4 independent experiments and analyzed using  
544 Student's t test). \* denotes p<0.05, \*\* denotes p<0.01, and \*\*\* denotes p<0.001 for all panels.  
545



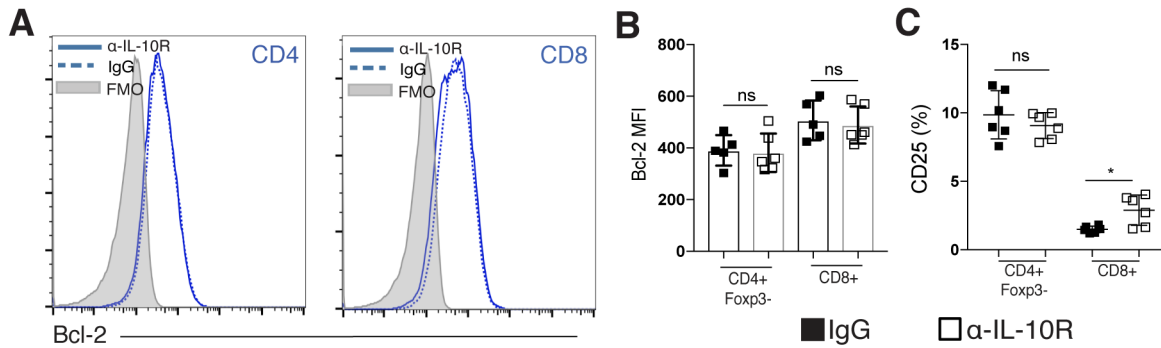
546  
547

548 **Figure 4. ICOSL blockade increases CD25 expression and STAT5 phosphorylation in**  
549 **effector T cells in the brain during chronic infection. (A-D)** T cells were isolated from the  
550 brains of chronically infected control or  $\alpha$ -ICOSL-treated mice. Representative flow plots of  
551 CD25+CD4+ effector T cells (A) and CD25+CD8+ effector T cells (C) are shown. Number in

552 gate indicates the mean frequency of CD25+ cells +/- standard error. **(B)** Total number of  
553 CD25+ CD4+ effector T cells and **(D)** total number of CD25+ CD8+ T cells isolated from the  
554 brain (n=4 per group, data is pooled from 3 independent experiments and analyzed by  
555 randomized block ANOVA). **(E-I)** Brain sections from chronically infected control **(E, H)** and  
556  $\alpha$ -ICOSL-treated **(F, I)** mice were stained for CD4 or CD8 (green), pSTAT5 (red) and DAPI  
557 (blue). White arrowheads indicate pSTAT5+ CD4 or CD8 T cells. **(G)** The number of  
558 pSTAT5+CD4+ and **(J)** number of pSTAT5+CD8+ T cells were quantified per 500  $\mu\text{m}^2$  (n=4-5  
559 mice per group, data is pooled from two independent experiments and analyzed using  
560 randomized block ANOVA). \* denotes  $p<0.05$ , \*\* denotes  $p<0.01$ , and \*\*\* denotes  $p<0.001$  for  
561 all panels.

562

563



564

565

**Figure 5. IL-10R blockade does not affect Bcl-2 or CD25 expression on T cells in the brain**

566

**during chronic infection.** (A-C) Effector T cell populations isolated from the brain were

567

analyzed by flow cytometry following  $\alpha$ -IL-10R blockade. (A) Representative histograms

568

showing Bcl-2 expression on effector CD4+ and CD8+ T cells isolated from the brains of

569

chronically infected mice treated with control or  $\alpha$ -IL-10R blocking antibody. (B) The MFI of

570

Bcl-2 on effector T cells isolated from the brains of control or  $\alpha$ -IL-10R-treated mice (n=5-6 per

571

group, data is representative of three independent experiments and analyzed using Student's t

572

test). (C) The frequency of CD25+ effector T cells isolated from the brains of chronically

573

infected mice after  $\alpha$ -IL-10R treatment (n= 6 per group, data is representative of two independent

574

experiments and analyzed using Student's t test). \* denotes  $p < 0.05$ , \*\* denotes  $p < 0.01$ , and \*\*\*

575

denotes  $p < 0.001$  for all panels.

576 **Acknowledgements**

577 The authors would like to thank all the members of the Harris lab and Center for Brain  
578 Immunology and Glia (BIG) for their insightful comments and discussion during the preparation  
579 of this work. We acknowledge support from the Research Histology core facility at the  
580 University of Virginia. We would also like to thank Marieke K. Jones for her helpful input  
581 regarding relevant statistical analysis and coding, and Dr. Ken Tung for his assistance with  
582 histopathological examination of tissue sections.

583 **Disclosures**

584 The authors have no financial conflicts of interest.

585

## 586 References

- 587 1. McKenzie, B.S., R.A. Kastelein, and D.J. Cua, *Understanding the IL-23-IL-17 immune pathway*.  
588 Trends Immunol, 2006. **27**(1): p. 17-23.
- 589 2. Medzhitov, R., *Recognition of microorganisms and activation of the immune response*. Nature,  
590 2007. **449**(7164): p. 819-26.
- 591 3. Gazzinelli, R., M. Wysocka, S. Hieny, T. Schariton-Kersten, A. Cheever, R. Kühn, W. Müller, G.  
592 Trinchieri, and A. Sher, *In the absence of endogenous IL-10, mice acutely infected with*  
593 *Toxoplasma gondii succumb to a lethal immune response dependent on CD4+ T cells and*  
594 *accompanied by overproduction of IL-12, IFN-gamma and TNF-alpha*. The Journal of  
595 Immunology, 1996. **157**(2): p. 798-805.
- 596 4. Couper, K.N., D.G. Blount, M.S. Wilson, J.C. Hafalla, Y. Belkaid, M. Kamanaka, R.A. Flavell,  
597 J.B. de Souza, and E.M. Riley, *IL-10 from CD4CD25Foxp3CD127 adaptive regulatory T cells*  
598 *modulates parasite clearance and pathology during malaria infection*. PLoS Pathog, 2008. **4**(2):  
599 p. e1000004.
- 600 5. Sun, J., R. Madan, C.L. Karp, and T.J. Braciale, *Effector T cells control lung inflammation during*  
601 *acute influenza virus infection by producing IL-10*. Nat Med, 2009. **15**(3): p. 277-84.
- 602 6. Belkaid, Y., C.A. Piccirillo, S. Mendez, E.M. Shevach, and D.L. Sacks, *CD4+CD25+ regulatory*  
603 *T cells control Leishmania major persistence and immunity*. Nature, 2002. **420**(6915): p. 502-  
604 507.
- 605 7. Villarino, A., L. Hibbert, L. Lieberman, E. Wilson, T. Mak, H. Yoshida, R.A. Kastelein, C. Saris,  
606 and C.A. Hunter, *The IL-27R (WSX-1) is required to suppress T cell hyperactivity during*  
607 *infection*. Immunity, 2003. **19**(5): p. 645-655.
- 608 8. Redford, P.S., P.J. Murray, and A. O'Garra, *The role of IL-10 in immune regulation during M.*  
609 *tuberculosis infection*. Mucosal Immunol, 2011. **4**(3): p. 261-70.
- 610 9. Couper, K.N., D.G. Blount, and E.M. Riley, *IL-10: the master regulator of immunity to infection*.  
611 Journal of immunology, 2008. **180**(9): p. 5771-7.
- 612 10. de Waal Malefyt, R., J. Haanen, H. Spits, M.G. Roncarolo, A. te Velde, C. Figdor, K. Johnson, R.  
613 Kastelein, H. Yssel, and J.E. de Vries, *Interleukin 10 (IL-10) and viral IL-10 strongly reduce*  
614 *antigen-specific human T cell proliferation by diminishing the antigen-presenting capacity of*  
615 *monocytes via downregulation of class II major histocompatibility complex expression*. J Exp  
616 Med, 1991. **174**(4): p. 915-24.
- 617 11. Fiorentino, D.F., A. Zlotnik, P. Vieira, T.R. Mosmann, M. Howard, K.W. Moore, and A. O'Garra,  
618 *IL-10 acts on the antigen-presenting cell to inhibit cytokine production by Th1 cells*. Journal of  
619 immunology, 1991. **146**(10): p. 3444-51.
- 620 12. Ding, L. and E.M. Shevach, *IL-10 inhibits mitogen-induced T cell proliferation by selectively*  
621 *inhibiting macrophage costimulatory function*. Journal of immunology, 1992. **148**(10): p. 3133-9.
- 622 13. de Waal Malefyt, R., H. Yssel, and J.E. de Vries, *Direct effects of IL-10 on subsets of human*  
623 *CD4+ T cell clones and resting T cells. Specific inhibition of IL-2 production and proliferation*.  
624 The Journal of Immunology, 1993. **150**(11): p. 4754-4765.
- 625 14. Taga, K. and G. Tosato, *IL-10 inhibits human T cell proliferation and IL-2 production*. Journal of  
626 immunology, 1992. **148**(4): p. 1143-8.
- 627 15. Dupont, C.D., D.A. Christian, and C.A. Hunter. *Immune response and immunopathology during*  
628 *toxoplasmosis*. in *Seminars in immunopathology*. 2012. Springer.
- 629 16. Dubey, J.P., *The history of Toxoplasma gondii--the first 100 years*. The Journal of eukaryotic  
630 microbiology, 2008. **55**(6): p. 467-75.
- 631 17. Saeij, J.P., J.P. Boyle, M.E. Grigg, G. Arrizabalaga, and J.C. Boothroyd, *Bioluminescence*  
632 *imaging of Toxoplasma gondii infection in living mice reveals dramatic differences between*  
633 *strains*. Infect Immun, 2005. **73**(2): p. 695-702.



- 634 18. Ricardo Gazzinelli, Y.X., Sara Hieny, Allen Cheever, Alan Sher, *Simultaneous depletion of*  
635 *CD4+ and CD8+ T lymphocytes is required to reactivate chronic infection with Toxoplasma*  
636 *gondii*. Journal of immunology, 1992. **149**(1): p. 175-180.
- 637 19. Yap, G., M. Pesin, and A. Sher, *Cutting Edge: IL-12 Is Required for the Maintenance of IFN-*  
638 *Production in T Cells Mediating Chronic Resistance to the Intracellular Pathogen, Toxoplasma*  
639 *gondii*. The Journal of Immunology, 2000. **165**(2): p. 628-631.
- 640 20. Ellis-Neyer, L., G. Grunig, M. Fort, J. Remington, D. Rennick, and C. Hunter, *Role of IL-10 in*  
641 *regulation of T-cell-dependent and T-cell-independent mechanism of resistance*. Infect. Immun,  
642 1997. **65**: p. 1675-1682.
- 643 21. Wilson, E.H., U. Wille-Reece, F. Dzierszynski, and C.A. Hunter, *A critical role for IL-10 in*  
644 *limiting inflammation during toxoplasmic encephalitis*. Journal of neuroimmunology, 2005.  
645 **165**(1): p. 63-74.
- 646 22. Hutloff, A., A.M. Dittrich, K.C. Beier, B. Eljaschewitsch, R. Kraft, I. Anagnostopoulos, and R.A.  
647 Kroczek, *ICOS is an inducible T-cell co-stimulator structurally and functionally related to CD28*.  
648 Nature, 1999. **402**: p. 21-24.
- 649 23. Simpson, T.R., S.A. Quezada, and J.P. Allison, *Regulation of CD4 T cell activation and effector*  
650 *function by inducible costimulator (ICOS)*. Curr Opin Immunol, 2010. **22**(3): p. 326-32.
- 651 24. Anthony J. Coyle, S.L., Clare Lloyd, Jane Tian, Tracy Delaney, Stephen Manning, Trang  
652 Nguyen, Tim Burwell, Helga Schneider, Jose Angel Gonzalo, Michael Gosselin, Laura Rudolph  
653 Owen, Christopher E. Rudd, Jose Carlos Gutierrez-Ramos, *The CD28-related molecule ICOS is*  
654 *required for effective T cell-dependent immune responses*. Immunity, 2000. **13**: p. 95-105.
- 655 25. Chen Dong, A.E.J., Ulla-Angela Temann, Sujan Shresta, James P. Allison, Nancy H. Ruddle,  
656 Richard A. Flavell, *ICOS co-stimulatory receptor is essential for T-cell activation and function*.  
657 Nature, 2001. **409**: p. 97-101.
- 658 26. Bossaller, L., J. Burger, R. Draeger, B. Grimbacher, R. Knoth, A. Plebani, A. Durandy, U.  
659 Baumann, M. Schlesier, and A.A. Welcher, *ICOS deficiency is associated with a severe reduction*  
660 *of CXCR5+ CD4 germinal center Th cells*. The Journal of Immunology, 2006. **177**(7): p. 4927-  
661 4932.
- 662 27. Carreno, B.M. and M. Collins, *The B7 family of ligands and its receptors: new pathways for*  
663 *costimulation and inhibition of immune responses*. Annual review of immunology, 2002. **20**: p.  
664 29-53.
- 665 28. Witsch, E.J., M. Peiser, A. Hutloff, K. Büchner, B.G. Dorner, H. Jonuleit, H.W. Mages, and R.A.  
666 Kroczek, *ICOS and CD28 reversely regulate IL - 10 on re - activation of human effector T cells*  
667 *with mature dendritic cells*. European journal of immunology, 2002. **32**(9): p. 2680-2686.
- 668 29. Villegas-Mendez, A., T.N. Shaw, C.A. Inkson, P. Strangward, J.B. de Souza, and K.N. Couper,  
669 *Parasite-Specific CD4+ IFN-γ+ IL-10+ T Cells Distribute within Both Lymphoid and*  
670 *Nonlymphoid Compartments and Are Controlled Systemically by Interleukin-27 and ICOS during*  
671 *Blood-Stage Malaria Infection*. Infection and immunity, 2016. **84**(1): p. 34-46.
- 672 30. Okamoto, N., K. Tezuka, M. Kato, R. Abe, and T. Tsuji, *PI3-kinase and MAP-kinase signaling*  
673 *cascades in AILIM/ICOS- and CD28-costimulated T-cells have distinct functions between cell*  
674 *proliferation and IL-10 production*. Biochem Biophys Res Commun, 2003. **310**(3): p. 691-702.
- 675 31. Smigiel, K.S., E. Richards, S. Srivastava, K.R. Thomas, J.C. Dudda, K.D. Klonowski, and D.J.  
676 Campbell, *CCR7 provides localized access to IL-2 and defines homeostatically distinct*  
677 *regulatory T cell subsets*. The Journal of experimental medicine, 2014. **211**(1): p. 121-136.
- 678 32. Raynor, J., R. Karns, M. Almanan, K.P. Li, S. Divanovic, C.A. Chougnet, and D.A. Hildeman,  
679 *IL-6 and ICOS Antagonize Bim and Promote Regulatory T Cell Accrual with Age*. Journal of  
680 immunology, 2015. **195**(3): p. 944-52.
- 681 33. Herman, A.E., G.J. Freeman, D. Mathis, and C. Benoist, *CD4+CD25+ T regulatory cells*  
682 *dependent on ICOS promote regulation of effector cells in the prediabetic lesion*. J Exp Med,  
683 2004. **199**(11): p. 1479-89.

- 684 34. Redpath, S.A., N. van der Werf, A.M. Cervera, A.S. MacDonald, D. Gray, R.M. Maizels, and  
685 M.D. Taylor, *ICOS controls Foxp3(+) regulatory T-cell expansion, maintenance and IL-10*  
686 *production during helminth infection*. Eur J Immunol, 2013. **43**(3): p. 705-15.
- 687 35. Villegas, E.N., L.A. Lieberman, N. Mason, S.L. Blass, V.P. Zediak, R. Peach, T. Horan, S.  
688 Yoshinaga, and C.A. Hunter, *A role for inducible costimulator protein in the CD28- independent*  
689 *mechanism of resistance to Toxoplasma gondii*. Journal of immunology, 2002. **169**(2): p. 937-43.
- 690 36. Wilson, E.H., C. Zaph, M. Mohrs, A. Welcher, J. Siu, D. Artis, and C.A. Hunter, *B7RP-1-ICOS*  
691 *Interactions Are Required for Optimal Infection-Induced Expansion of CD4+ Th1 and Th2*  
692 *Responses*. The Journal of Immunology, 2006. **177**(4): p. 2365-2372.
- 693 37. Glatman Zaretsky, A., J.S. Silver, M. Siwicki, A. Durham, C.F. Ware, and C.A. Hunter, *Infection*  
694 *with Toxoplasma gondii alters lymphotoxin expression associated with changes in splenic*  
695 *architecture*. Infect Immun, 2012. **80**(10): p. 3602-10.
- 696 38. O'Brien, C.A., C. Overall, C. Konradt, A.C. O'Hara Hall, N.W. Hayes, S. Wagage, B. John, D.A.  
697 Christian, C.A. Hunter, and T.H. Harris, *CD11c-Expressing Cells Affect Regulatory T Cell*  
698 *Behavior in the Meninges during Central Nervous System Infection*. The Journal of Immunology,  
699 2017.
- 700 39. Roers, A., L. Siewe, E. Strittmatter, M. Deckert, D. Schlüter, W. Stenzel, A.D. Gruber, T. Krieg,  
701 K. Rajewsky, and W. Müller, *T cell-specific inactivation of the interleukin 10 gene in mice*  
702 *results in enhanced T cell responses but normal innate responses to lipopolysaccharide or skin*  
703 *irritation*. Journal of Experimental Medicine, 2004. **200**(10): p. 1289-1297.
- 704 40. Jankovic, D., M.C. Kullberg, C.G. Feng, R.S. Goldszmid, C.M. Collazo, M. Wilson, T.A. Wynn,  
705 M. Kamanaka, R.A. Flavell, and A. Sher, *Conventional T-bet+ Foxp3- Th1 cells are the major*  
706 *source of host-protective regulatory IL-10 during intracellular protozoan infection*. The Journal  
707 of experimental medicine, 2007. **204**(2): p. 273-283.
- 708 41. Ricardo Gazzinelli, M.W., Sara Hieny, Tanya Scharton-Kersten, Allen Cheever, Ralf Kuhn,  
709 Werner Muller, Giorgio Trinchieri, Alan Sher, *In the absense of endogenous IL-10, mice acutely*  
710 *infected with Toxoplasma gondii succumb to a lethal immune response dependent on CD4+ T*  
711 *cells and accompanied by overproduction of IL-12, IFN-g, and TNF-a*. Journal of immunology,  
712 1996. **96**: p. 798-805.
- 713 42. Sturge, C.R. and F. Yarovinsky, *Complex immune cell interplay in the gamma interferon*  
714 *response during Toxoplasma gondii infection*. Infect Immun, 2014. **82**(8): p. 3090-7.
- 715 43. Stumhofer, J.S., A. Laurence, E.H. Wilson, E. Huang, C.M. Tato, L.M. Johnson, A.V. Villarino,  
716 Q. Huang, A. Yoshimura, and D. Sehly, *Interleukin 27 negatively regulates the development of*  
717 *interleukin 17-producing T helper cells during chronic inflammation of the central nervous*  
718 *system*. Nature immunology, 2006. **7**(9): p. 937-945.
- 719 44. Stumhofer, J.S., J.S. Silver, A. Laurence, P.M. Porrett, T.H. Harris, L.A. Turka, M. Ernst, C.J.  
720 Saris, J.J. O'Shea, and C.A. Hunter, *Interleukins 27 and 6 induce STAT3-mediated T cell*  
721 *production of interleukin 10*. Nature immunology, 2007. **8**(12): p. 1363-1371.
- 722 45. Laan, M., Z.H. Cui, H. Hoshino, J. Lotvall, M. Sjostrand, D.C. Gruenert, B.E. Skoogh, and A.  
723 Linden, *Neutrophil recruitment by human IL-17 via C-X-C chemokine release in the airways*.  
724 Journal of immunology, 1999. **162**(4): p. 2347-52.
- 725 46. Hoshino, H., M. Laan, M. Sjostrand, J. Lotvall, B.E. Skoogh, and A. Linden, *Increased elastase*  
726 *and myeloperoxidase activity associated with neutrophil recruitment by IL-17 in airways in vivo*.  
727 J Allergy Clin Immunol, 2000. **105**(1 Pt 1): p. 143-9.
- 728 47. Kelly, M.N., J.K. Kolls, K. Happel, J.D. Schwartzman, P. Schwarzenberger, C. Combe, M.  
729 Moretto, and I.A. Khan, *Interleukin-17/interleukin-17 receptor-mediated signaling is important*  
730 *for generation of an optimal polymorphonuclear response against Toxoplasma gondii infection*.  
731 Infect Immun, 2005. **73**(1): p. 617-21.
- 732 48. Roussel, L., F. Houle, C. Chan, Y. Yao, J. Berube, R. Olivenstein, J.G. Martin, J. Huot, Q.  
733 Hamid, L. Ferri, and S. Rousseau, *IL-17 promotes p38 MAPK-dependent endothelial activation*

- 734 *enhancing neutrophil recruitment to sites of inflammation*. Journal of immunology, 2010. **184**(8):  
735 p. 4531-7.
- 736 49. De Filippo, K., A. Dudeck, M. Hasenberg, E. Nye, N. van Rooijen, K. Hartmann, M. Gunzer, A.  
737 Roers, and N. Hogg, *Mast cell and macrophage chemokines CXCL1/CXCL2 control the early*  
738 *stage of neutrophil recruitment during tissue inflammation*. Blood, 2013. **121**(24): p. 4930-7.
- 739 50. Grist, J.J., B.S. Marro, D.D. Skinner, A.R. Syage, C. Worne, D.J. Doty, R.S. Fujinami, and T.E.  
740 Lane, *Induced CNS expression of CXCL1 augments neurologic disease in a murine model of*  
741 *multiple sclerosis via enhanced neutrophil recruitment*. Eur J Immunol, 2018. **48**(7): p. 1199-  
742 1210.
- 743 51. Gelderblom, M., A. Weymar, C. Bernreuther, J. Velden, P. Arunachalam, K. Steinbach, E.  
744 Orthey, T.V. Arumugam, F. Leypoldt, O. Simova, V. Thom, M.A. Friese, I. Prinz, C. Holscher,  
745 M. Glatzel, T. Korn, C. Gerloff, E. Tolosa, and T. Magnus, *Neutralization of the IL-17 axis*  
746 *diminishes neutrophil invasion and protects from ischemic stroke*. Blood, 2012. **120**(18): p. 3793-  
747 802.
- 748 52. Kim, J.V., S.S. Kang, M.L. Dustin, and D.B. McGavern, *Myelomonocytic cell recruitment causes*  
749 *fatal CNS vascular injury during acute viral meningitis*. Nature, 2009. **457**(7226): p. 191-5.
- 750 53. McAdam, A.J., R.J. Greenwald, M.A. Levin, T. Chernova, N. Malenkovich, V. Ling, G.J.  
751 Freeman, and A.H. Sharpe, *ICOS is critical for CD40-mediated antibody class switching*. Nature,  
752 2001. **409**(6816): p. 102-105.
- 753 54. Bentebibel, S.E., S. Lopez, G. Obermoser, N. Schmitt, C. Mueller, C. Harrod, E. Flano, A.  
754 Mejias, R.A. Albrecht, D. Blankenship, H. Xu, V. Pascual, J. Banchereau, A. Garcia-Sastre, A.K.  
755 Palucka, O. Ramilo, and H. Ueno, *Induction of ICOS+CXCR3+CXCR5+ TH cells correlates with*  
756 *antibody responses to influenza vaccination*. Science translational medicine, 2013. **5**(176): p.  
757 176ra32.
- 758 55. Malek, T.R. and I. Castro, *Interleukin-2 receptor signaling: at the interface between tolerance*  
759 *and immunity*. Immunity, 2010. **33**(2): p. 153-165.
- 760 56. Boyman, O. and J. Sprent, *The role of interleukin-2 during homeostasis and activation of the*  
761 *immune system*. Nature reviews. Immunology, 2012. **12**(3): p. 180-90.
- 762 57. Alejandro Villarino, L.H., Linda Lieberman, Emma Wilson, Tak Mak, Hiroki Yoshida, Robert A.  
763 Kastelein, Christiaan Saris, Christopher A. Hunter, *The IL-27R (WSX-1) is required to suppress T*  
764 *cell hyperactivity during infection*. Immunity, 2003. **19**: p. 645-655.
- 765 58. Yong, P.F., U. Salzer, and B. Grimbacher, *The role of costimulation in antibody deficiencies:*  
766 *ICOS and common variable immunodeficiency*. Immunol Rev, 2009. **229**(1): p. 101-13.
- 767 59. Warnatz, K., L. Bossaller, U. Salzer, A. Skrabl-Baumgartner, W. Schwinger, M. van der Burg,  
768 J.J. van Dongen, M. Orłowska-Volk, R. Knoth, A. Durandy, R. Draeger, M. Schlesier, H.H.  
769 Peter, and B. Grimbacher, *Human ICOS deficiency abrogates the germinal center reaction and*  
770 *provides a monogenic model for common variable immunodeficiency*. Blood, 2006. **107**(8): p.  
771 3045-52.
- 772 60. Grimbacher, B., A. Hutloff, M. Schlesier, E. Glocker, K. Warnatz, R. Dräger, H. Eibel, B.  
773 Fischer, A.A. Schaffer, H.W. Mages, R.A. Kroczeck, and H.H. Peter, *Homozygous loss of ICOS is*  
774 *associated with adult-onset common variable immunodeficiency*. Nat Immunol, 2003. **4**(3): p.  
775 261-8.
- 776 61. Giovannetti, A., M. Pierdominici, F. Mazzetta, M. Marziali, C. Renzi, A.M. Mileo, M. De Felice,  
777 B. Mora, A. Esposito, R. Carello, A. Pizzuti, M.G. Paggi, R. Paganelli, W. Malorni, and F. Aiuti,  
778 *Unravelling the complexity of T cell abnormalities in common variable immunodeficiency*.  
779 Journal of immunology, 2007. **178**(6): p. 3932-43.
- 780 62. Cunningham-Rundles, C. and C. Bodian, *Common variable immunodeficiency: clinical and*  
781 *immunological features of 248 patients*. Clin Immunol, 1999. **92**(1): p. 34-48.
- 782 63. Cunningham-Rundles, C., *Autoimmune manifestations in common variable immunodeficiency*. J  
783 Clin Immunol, 2008. **28 Suppl 1**: p. S42-5.

- 784 64. Moore, K.W., R. de Waal Malefyt, R.L. Coffman, and A. O'Garra, *Interleukin-10 and the*  
785 *interleukin-10 receptor*. Annual review of immunology, 2001. **19**: p. 683-765.
- 786 65. Weber-Nordt, R.M., M.A. Meraz, and R.D. Schreiber, *Lipopolysaccharide-dependent induction*  
787 *of IL-10 receptor expression on murine fibroblasts*. Journal of immunology, 1994. **153**(8): p.  
788 3734-44.
- 789 66. Krakauer, T., *IL-10 inhibits the adhesion of leukocytic cells to IL-1-activated human endothelial*  
790 *cells*. Immunol Lett, 1995. **45**(1-2): p. 61-5.
- 791 67. John, B., B. Ricart, E.D.T. Wojno, T.H. Harris, L.M. Randall, D.A. Christian, B. Gregg, D.M. De  
792 Almeida, W. Weninger, and D.A. Hammer, *Analysis of behavior and trafficking of dendritic cells*  
793 *within the brain during toxoplasmic encephalitis*. PLoS pathogens, 2011. **7**(9): p. e1002246.
- 794 68. Smith, L.K., G.M. Boukhalel, S.A. Condotta, S. Mazouz, J.J. Guthmiller, R. Vijay, N.S. Butler,  
795 J. Bruneau, N.H. Shoukry, C.M. Krawczyk, and M.J. Richer, *Interleukin-10 Directly Inhibits*  
796 *CD8(+) T Cell Function by Enhancing N-Glycan Branching to Decrease Antigen Sensitivity*.  
797 Immunity, 2018. **48**(2): p. 299-312 e5.
- 798 69. Parry, R.V., J.M. Chemnitz, K.A. Frauwirth, A.R. Lanfranco, I. Braunstein, S.V. Kobayashi, P.S.  
799 Linsley, C.B. Thompson, and J.L. Riley, *CTLA-4 and PD-1 receptors inhibit T-cell activation by*  
800 *distinct mechanisms*. Mol Cell Biol, 2005. **25**(21): p. 9543-53.
- 801 70. Fife, B.T. and J.A. Bluestone, *Control of peripheral T-cell tolerance and autoimmunity via the*  
802 *CTLA-4 and PD-1 pathways*. Immunol Rev, 2008. **224**: p. 166-82.
- 803 71. Parry, R.V., C.A. Rumbley, L.H. Vandenberghe, C.H. June, and J.L. Riley, *CD28 and inducible*  
804 *costimulatory protein Src homology 2 binding domains show distinct regulation of*  
805 *phosphatidylinositol 3-kinase, Bcl-xL, and IL-2 expression in primary human CD4 T*  
806 *lymphocytes*. The Journal of immunology, 2003. **171**(1): p. 166-174.
- 807 72. Wikenheiser, D.J. and J.S. Stumhofer, *ICOS Co-Stimulation: Friend or Foe?* Frontiers in  
808 Immunology, 2016. **7**(304).
- 809 73. Jones, R.G., A.R. Elford, M.J. Parsons, L. Wu, C.M. Krawczyk, W.C. Yeh, R. Hakem, R.  
810 Rottapel, J.R. Woodgett, and P.S. Ohashi, *CD28-dependent activation of protein kinase B/Akt*  
811 *blocks Fas-mediated apoptosis by preventing death-inducing signaling complex assembly*. J Exp  
812 Med, 2002. **196**(3): p. 335-48.
- 813 74. Jones, R.G. and C.B. Thompson, *Revvng the engine: signal transduction fuels T cell activation*.  
814 Immunity, 2007. **27**(2): p. 173-8.
- 815 75. Parsons, M.J., R.G. Jones, M.S. Tsao, B. Odermatt, P.S. Ohashi, and J.R. Woodgett, *Expression*  
816 *of active protein kinase B in T cells perturbs both T and B cell homeostasis and promotes*  
817 *inflammation*. Journal of immunology, 2001. **167**(1): p. 42-8.
- 818 76. Kim, E.H., J.A. Sullivan, E.H. Plisch, M.M. Tejera, A. Jatzek, K.Y. Choi, and M. Suresh, *Signal*  
819 *integration by Akt regulates CD8 T cell effector and memory differentiation*. Journal of  
820 immunology, 2012. **188**(9): p. 4305-14.
- 821 77. Hand, T.W., W. Cui, Y.W. Jung, E. Sefik, N.S. Joshi, A. Chandele, Y. Liu, and S.M. Kaech,  
822 *Differential effects of STAT5 and PI3K/AKT signaling on effector and memory CD8 T-cell*  
823 *survival*. Proceedings of the National Academy of Sciences of the United States of America,  
824 2010. **107**(38): p. 16601-6.
- 825